

Rare hyperon decays as probes of BSM physics

Jusak Tandean

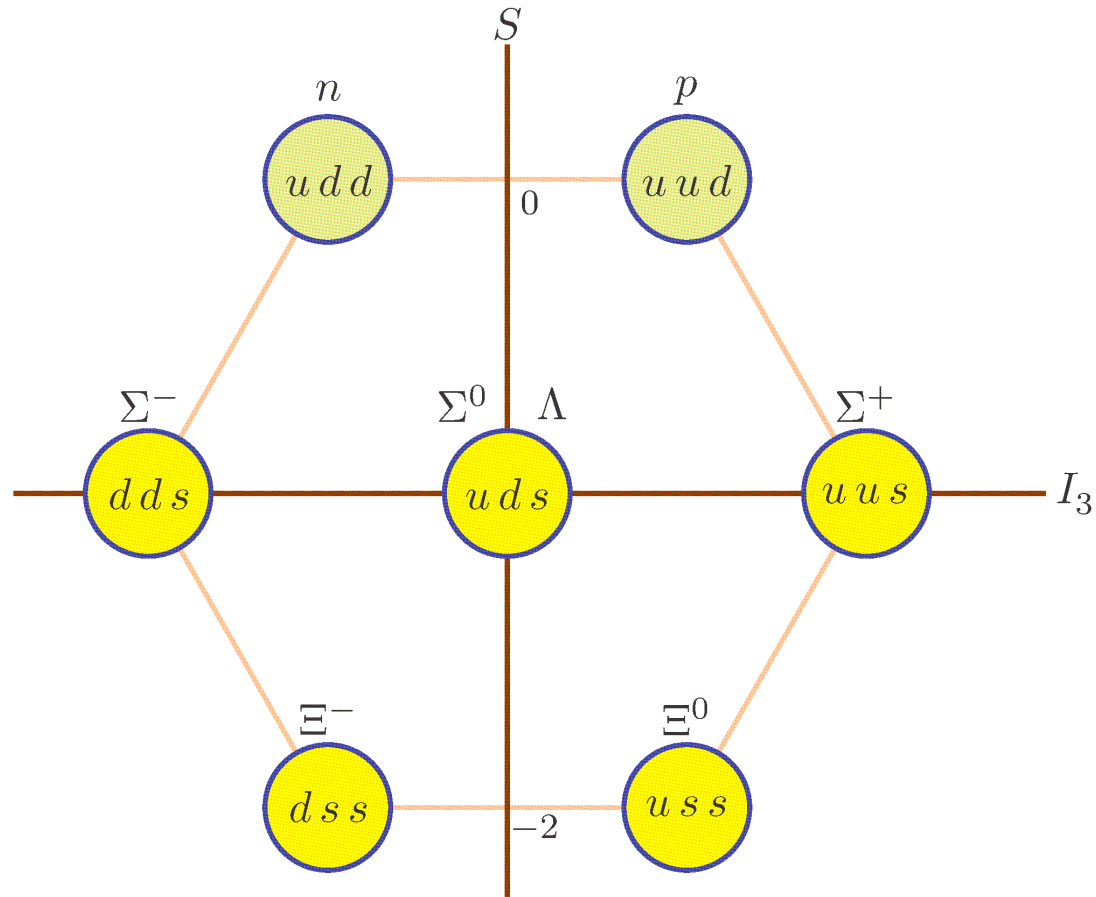
National Taiwan University

POST FPCP 2018 WORKSHOP
IITH, Hyderabad, India

21 July 2018

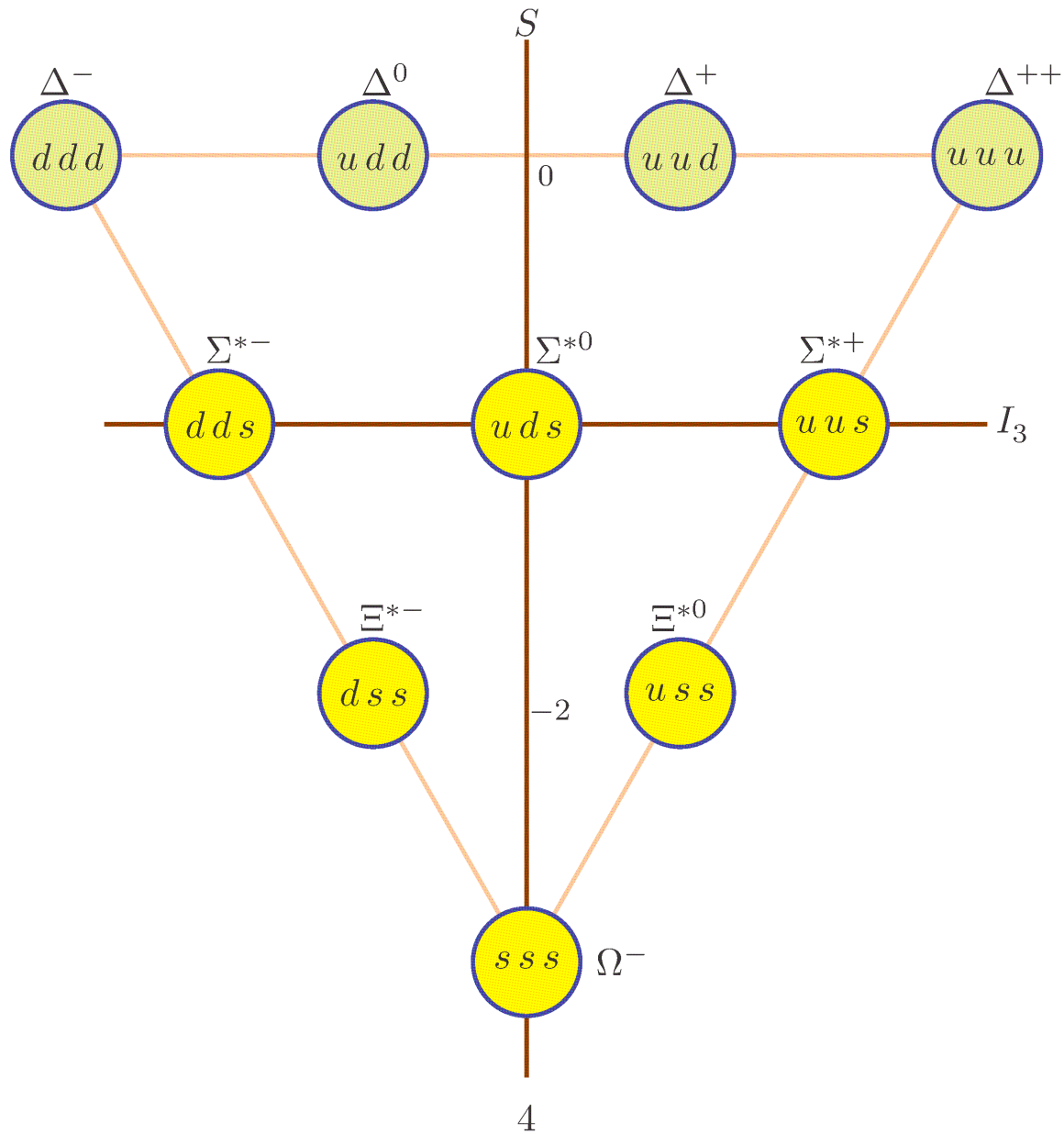
Lightest baryons

- Flavor-SU(3)-octet spin-1/2 baryons



Lightest baryons

- Flavor-SU(3)-decuplet spin-3/2 baryons



Rare hyperon decays

- They often involve flavor-changing neutral currents.
- Some of these decays cannot occur in the SM.
- Hence these processes are potentially sensitive to the effects of physics beyond the SM.
- Constraints from these decays complement the constraints from the kaon sector.
 - Operators contributing to $K \rightarrow \mu^+ \mu^-$ and $K \rightarrow \pi \mu^+ \mu^-$ also affect $\Sigma^+ \rightarrow p \mu^+ \mu^-$.

- Introduction
- $\Sigma^+ \rightarrow p \mu^+ \mu^-$
- Flavor-changing baryon decay $\mathcal{B} \rightarrow \mathcal{B}' \nu \nu$
- Lepton-number-violating $\mathcal{B}^- \rightarrow \mathcal{B}'^+ \ell^- \ell^-$
- Conclusions

Introduction

- $\Sigma^+ \rightarrow p \mu^+ \mu^-$

Flavor-changing baryon decay $\mathcal{B} \rightarrow \mathcal{B}' \nu \nu$

Lepton-number-violating $\mathcal{B}^- \rightarrow \mathcal{B}'^+ \ell^- \ell^-$

Conclusions

Evidence for the Decay $\Sigma^+ \rightarrow p\mu^+\mu^-$

H. K. Park,⁸ R. A. Burnstein,⁵ A. Chakravorty,⁵ Y. C. Chen,¹ W. S. Choong,^{2,7} K. Clark,⁹ E. C. Dukes,¹⁰ C. Durandet,¹⁰
 J. Felix,⁴ Y. Fu,⁷ G. Gidal,⁷ H. R. Gustafson,⁸ T. Holmstrom,¹⁰ M. Huang,¹⁰ C. James,³ C. M. Jenkins,⁹ T. Jones,⁷
 D. M. Kaplan,⁵ L. M. Lederman,⁵ N. Leros,⁶ M. J. Longo,^{8,*} F. Lopez,⁸ L. C. Lu,¹⁰ W. Luebke,⁵ K. B. Luk,^{2,7}
 K. S. Nelson,¹⁰ J.-P. Perroud,⁶ D. Rajaram,⁵ H. A. Rubin,⁵ J. Volk,³ C. G. White,⁵ S. L. White,⁵ and P. Zyla⁷

(HyperCP Collaboration)

¹*Institute of Physics, Academia Sinica, Taipei 11529, Taiwan, Republic of China*

²*University of California, Berkeley, California 94720, USA*

³*Fermi National Accelerator Laboratory, Batavia, Illinois 60510, USA*

⁴*Universidad de Guanajuato, 37000 León, Mexico*

⁵*Illinois Institute of Technology, Chicago, Illinois 60616, USA*

⁶*Université de Lausanne, CH-1015 Lausanne, Switzerland*

⁷*Lawrence Berkeley National Laboratory, Berkeley, California 94720, USA*

⁸*University of Michigan, Ann Arbor, Michigan 48109, USA*

⁹*University of South Alabama, Mobile, Alabama 36688, USA*

¹⁰*University of Virginia, Charlottesville, Virginia 22904, USA*

(Received 3 November 2004; published 18 January 2005)

We report the first evidence for the decay $\Sigma^+ \rightarrow p\mu^+\mu^-$ from data taken by the HyperCP (E871) experiment at Fermilab. Based on three observed events, the branching ratio is $\mathcal{B}(\Sigma^+ \rightarrow p\mu^+\mu^-) = [8.6_{-5.4}^{+6.6}(\text{stat}) \pm 5.5(\text{syst})] \times 10^{-8}$. The narrow range of dimuon masses may indicate that the decay proceeds via a neutral intermediate state, $\Sigma^+ \rightarrow pP^0, P^0 \rightarrow \mu^+\mu^-$ with a P^0 mass of $214.3 \pm 0.5 \text{ MeV}/c^2$ and branching ratio $\mathcal{B}(\Sigma^+ \rightarrow pP^0, P^0 \rightarrow \mu^+\mu^-) = [3.1_{-1.9}^{+2.4}(\text{stat}) \pm 1.5(\text{syst})] \times 10^{-8}$.

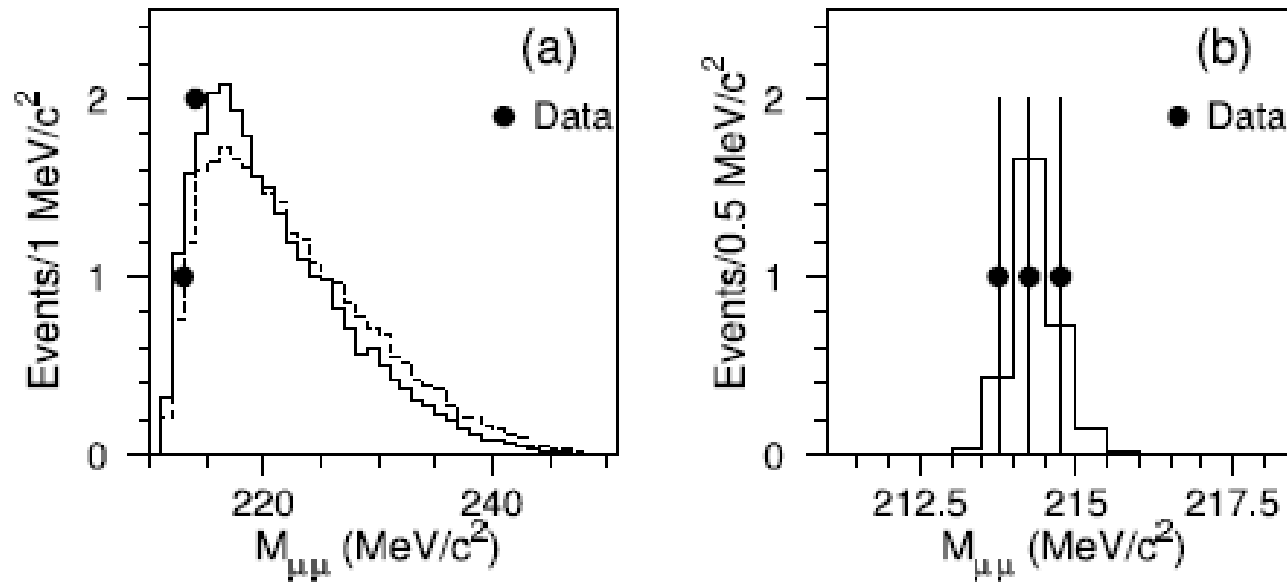



FIG. 4. Real (points) and MC (histogram) dimuon mass distributions for (a) $\Sigma_{\rho\mu\mu}^+$ MC events (arbitrary normalization) with a form-factor decay (solid histogram) and uniform phase-space decay (dashed histogram) model, and (b) $\Sigma_{\rho P\mu\mu}^+$ MC events normalized to match the data.

Evidence for the Rare Decay $\Sigma^+ \rightarrow p\mu^+\mu^-$

R. Aaij *et al.**
(LHCb Collaboration)

 (Received 22 December 2017; published 31 May 2018)

A search for the rare decay $\Sigma^+ \rightarrow p\mu^+\mu^-$ is performed using pp collision data recorded by the LHCb experiment at center-of-mass energies $\sqrt{s} = 7$ and 8 TeV, corresponding to an integrated luminosity of 3 fb^{-1} . An excess of events is observed with respect to the background expectation, with a signal significance of 4.1 standard deviations. No significant structure is observed in the dimuon invariant mass distribution, in contrast with a previous result from the HyperCP experiment. The measured $\Sigma^+ \rightarrow p\mu^+\mu^-$ branching fraction is $(2.2_{-1.3}^{+1.8}) \times 10^{-8}$, where statistical and systematic uncertainties are included, which is consistent with the standard model prediction.

A signal yield of $10.2_{-3.5}^{+3.9}$ is observed.

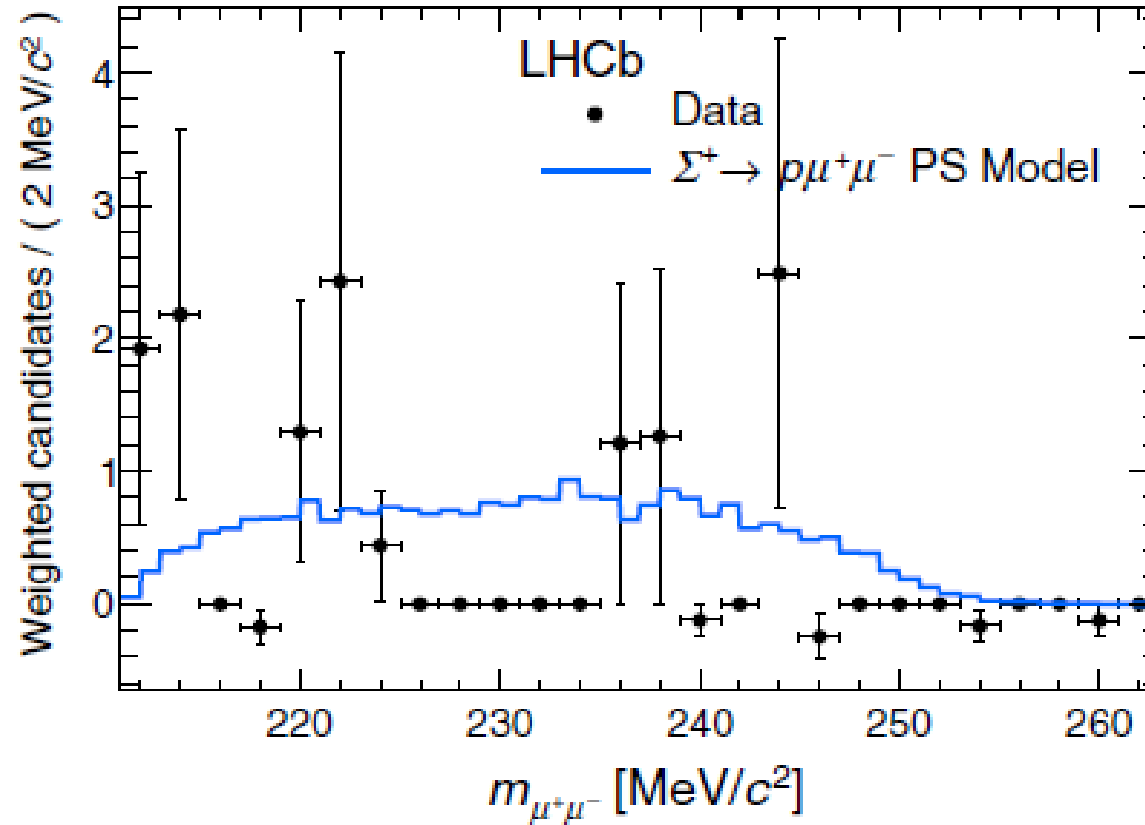
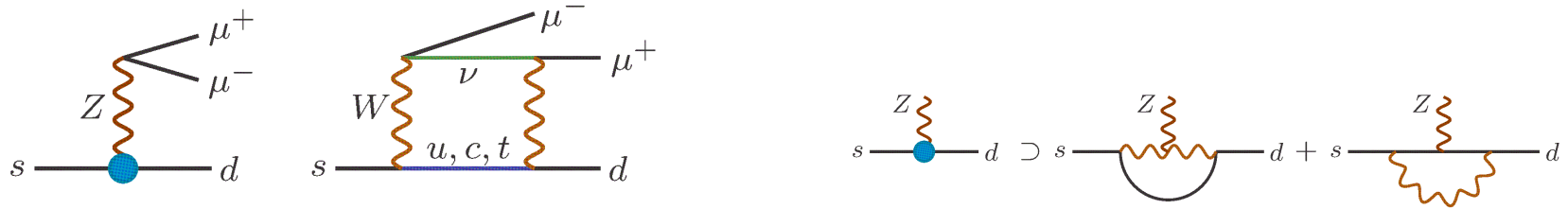


FIG. 3. Background-subtracted distribution of the dimuon invariant mass for $\Sigma^+ \rightarrow p\mu^+\mu^-$ candidates, superimposed with the distribution from the simulated phase-space (PS) model. Uncertainties on data points are calculated as the square root of the sum of squared weights.

$$\Sigma^+ \rightarrow p \mu^+ \mu^-$$

- The decay amplitude consists of short-distance & long-distance parts.
- The SM short-distance contribution arises mainly from Z-penguin and box diagrams



- It's described by the effective Hamiltonian

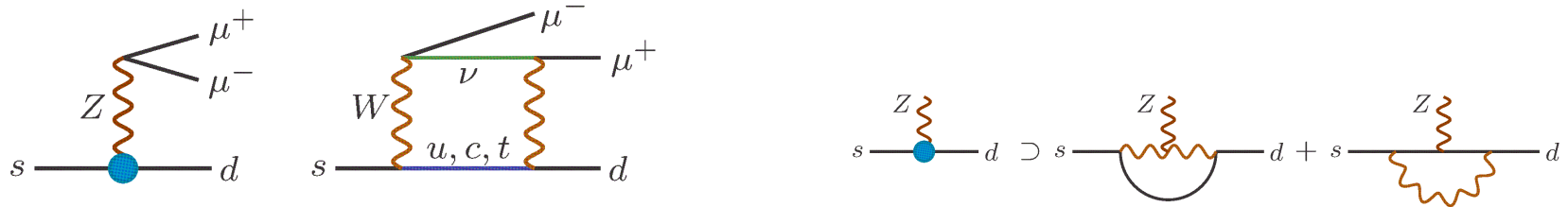
$$\mathcal{H}_{\text{eff}} = \frac{G_F}{\sqrt{2}} \bar{d} \gamma^\kappa (1 - \gamma_5) s \bar{\mu} \gamma_\kappa (\lambda_u z_{7V} - \lambda_t y_{7V} - \gamma_5 \lambda_t y_{7A}) \mu + \text{H.c.}$$

Buchalla, Buras, Lautenbacher, 1996

with Wilson coefficients z_{7V} & $y_{7V,7A}$ and CKM factor $\lambda_q = V_{qd}^* V_{qs}$

$$\Sigma^+ \rightarrow p \mu^+ \mu^-$$

- The decay amplitude consists of short-distance & long-distance parts.
- The SM short-distance contribution arises mainly from Z-penguin and box diagrams



- It's described by the effective Hamiltonian

$$\mathcal{H}_{\text{eff}} = \frac{G_F}{\sqrt{2}} \bar{d} \gamma^\kappa (1 - \gamma_5) s \bar{\mu} \gamma_\kappa (\lambda_u z_{7V} - \lambda_t y_{7V} - \gamma_5 \lambda_t y_{7A}) \mu + \text{H.c.}$$

Buchalla, Buras, Lautenbacher, 1996

with Wilson coefficients z_{7V} & $y_{7V,7A}$ and CKM factor $\lambda_q = V_{qd}^* V_{qs}$

- Hadronic matrix elements

$$\langle p | \bar{d} \gamma^\kappa s | \Sigma^+ \rangle = -\bar{u}_p \gamma^\kappa u_\Sigma,$$

$$\langle p | \bar{d} \gamma^\nu \gamma_5 s | \Sigma^+ \rangle = (D - F) \left(\bar{u}_p \gamma^\nu \gamma_5 u_\Sigma + \frac{m_\Sigma + m_p}{q^2 - m_K^2} \bar{u}_p \gamma_5 u_\Sigma q^\nu \right)$$

- The SM SD contribution alone yields a branching fraction of order 10^{-12}

- much smaller than the measured value, $\sim 2 \times 10^{-8}$

He, JT, Valencia, 2005

$$\Sigma^+ \rightarrow p \mu^+ \mu^-$$

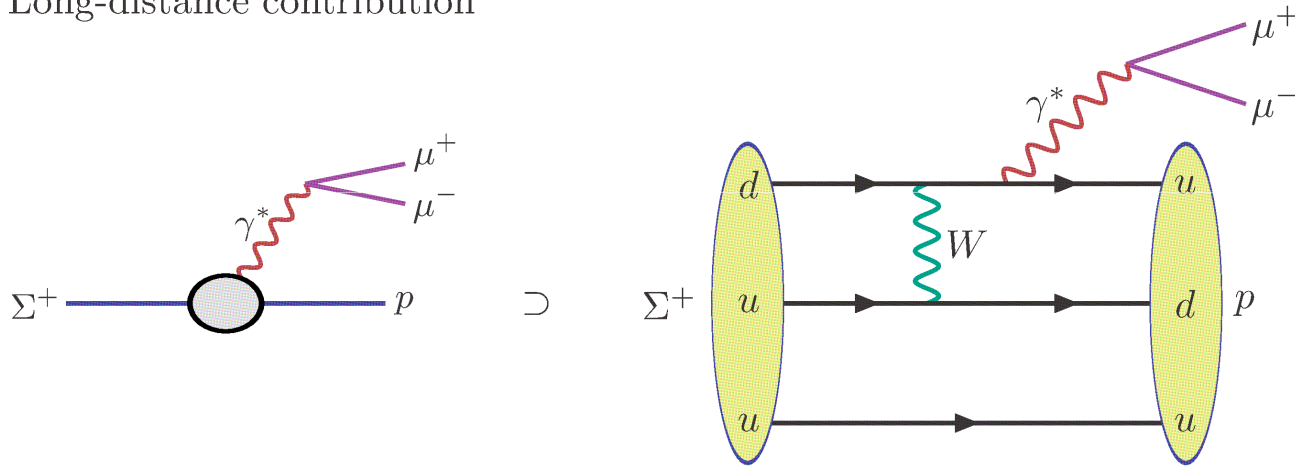
- Long-distance contribution mainly from $\Sigma^+ \rightarrow p \gamma^* \rightarrow p \mu^+ \mu^-$

$$\mathcal{M}_{\text{SM}}^{\text{LD}} = \frac{-ie^2 G_{\text{F}}}{q^2} \bar{u}_p (a + \gamma_5 b) \sigma_{\kappa\nu} q^\kappa u_\Sigma \bar{u}_\mu \gamma^\nu v_{\bar{\mu}} - e^2 G_{\text{F}} \bar{u}_p \gamma_\kappa (c + \gamma_5 d) u_\Sigma \bar{u}_\mu \gamma^\kappa v_{\bar{\mu}}$$

a, b, c, d are form factors depending on $q^2 = M_{\mu\mu}^2$

Lyagin & Ginzburg, 1962
Bergstrom, Safadi, Singer, 1988
He, JT, Valencia, 2005

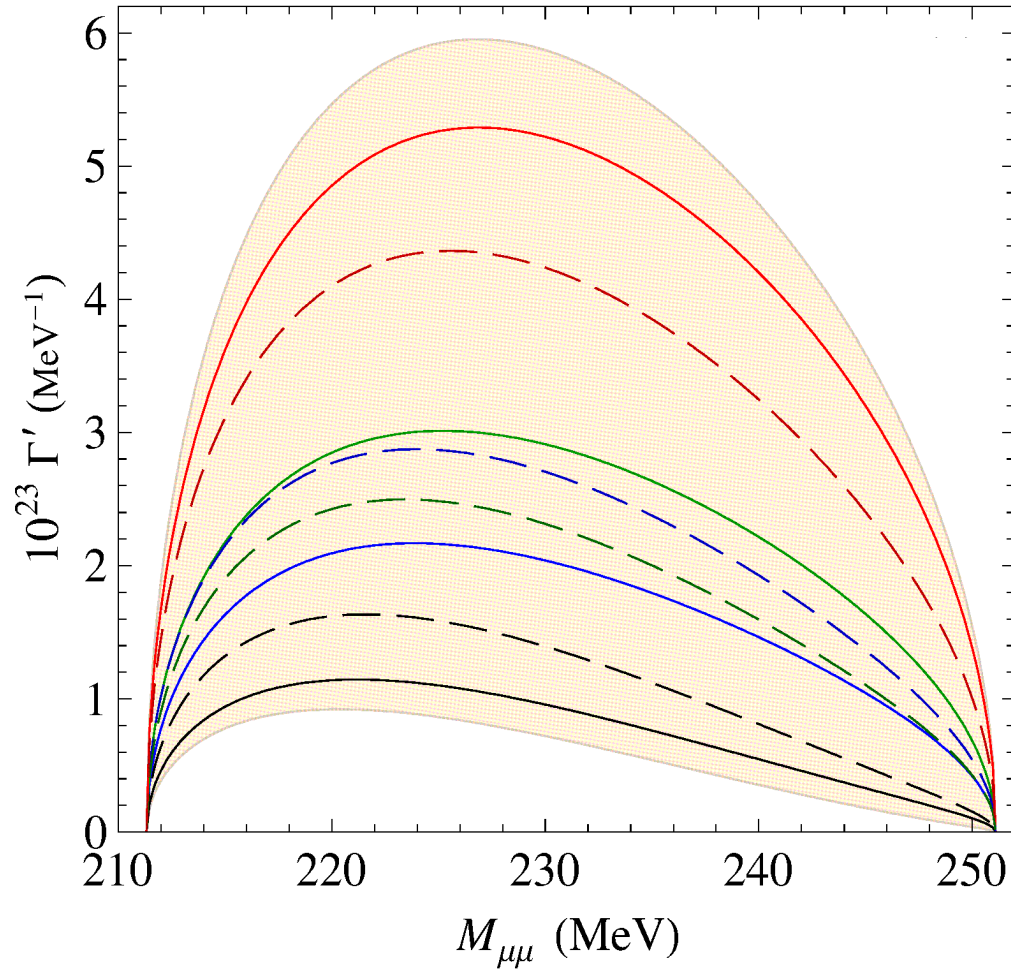
Long-distance contribution



- The LD contribution leads to significant uncertainties in the predicted rate.

Differential rate of $\Sigma^+ \rightarrow p\mu^+\mu^-$ in SM

• $\Gamma' = d\Gamma(\Sigma^+ \rightarrow p\mu^+\mu^-)/dq^2$



He, JT, Valencia, 1806.08350

Branching fraction of $\Sigma^+ \rightarrow p\mu^+\mu^-$ in SM

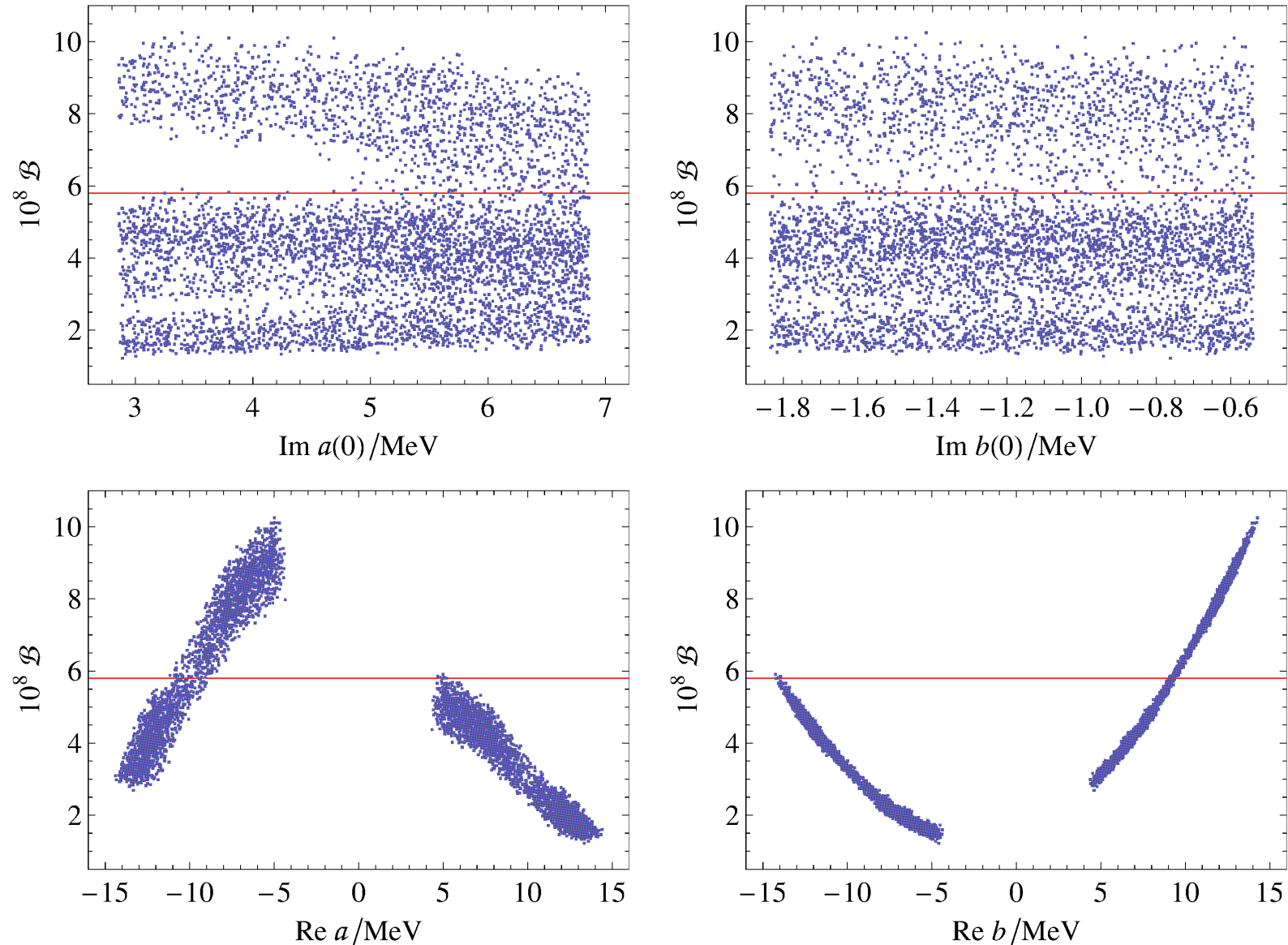


FIG. 1: Sample points of $\mathcal{B}(\Sigma^+ \rightarrow p\mu^+\mu^-) \times 10^8$ in relation to the preferred ranges of $\text{Im}(a, b)$ at $q^2 = 0$ and of $\text{Re}(a, b)$, as explained in the text. Each horizontal red line marks the 2σ upper-limit of the LHCb measurement [2].

◆ Amplitude accommodating SM and potential NP contributions

$$\begin{aligned} \mathcal{M} = & \bar{u}_p [i q_\kappa (\tilde{\mathbf{A}} + \gamma_5 \tilde{\mathbf{B}}) \sigma^{\nu\kappa} - \gamma^\nu (\tilde{\mathbf{C}} + \gamma_5 \tilde{\mathbf{D}})] u_\Sigma \bar{u}_\mu \gamma_\nu v_{\bar{\mu}} + \bar{u}_p \gamma^\nu (\tilde{\mathbf{E}} + \gamma_5 \tilde{\mathbf{F}}) u_\Sigma \bar{u}_\mu \gamma_\nu \gamma_5 v_{\bar{\mu}} \\ & + \bar{u}_p (\tilde{\mathbf{G}} + \gamma_5 \tilde{\mathbf{H}}) u_\Sigma \bar{u}_\mu v_{\bar{\mu}} + \bar{u}_p (\tilde{\mathbf{J}} + \gamma_5 \tilde{\mathbf{K}}) u_\Sigma \bar{u}_\mu \gamma_5 v_{\bar{\mu}} \end{aligned}$$

$\tilde{\mathbf{A}}, \tilde{\mathbf{B}}, \dots, \tilde{\mathbf{K}}$ are complex coefficients

◆ Amplitude accommodating SM and potential NP contributions

$$\begin{aligned} \mathcal{M} = & \bar{u}_p [iq_\kappa (\tilde{\mathbf{A}} + \gamma_5 \tilde{\mathbf{B}}) \sigma^{\nu\kappa} - \gamma^\nu (\tilde{\mathbf{C}} + \gamma_5 \tilde{\mathbf{D}})] u_\Sigma \bar{u}_\mu \gamma_\nu v_{\bar{\mu}} + \bar{u}_p \gamma^\nu (\tilde{\mathbf{E}} + \gamma_5 \tilde{\mathbf{F}}) u_\Sigma \bar{u}_\mu \gamma_\nu \gamma_5 v_{\bar{\mu}} \\ & + \bar{u}_p (\tilde{\mathbf{G}} + \gamma_5 \tilde{\mathbf{H}}) u_\Sigma \bar{u}_\mu v_{\bar{\mu}} + \bar{u}_p (\tilde{\mathbf{J}} + \gamma_5 \tilde{\mathbf{K}}) u_\Sigma \bar{u}_\mu \gamma_5 v_{\bar{\mu}} \end{aligned}$$

$\tilde{\mathbf{A}}, \tilde{\mathbf{B}}, \dots, \tilde{\mathbf{K}}$ are complex coefficients

● SM contributions

$$\tilde{\mathbf{A}} = \frac{e^2 G_F a}{q^2},$$

$$\tilde{\mathbf{B}} = \frac{e^2 G_F b}{q^2},$$

$$\tilde{\mathbf{C}} = e^2 G_F c + G_F \frac{\lambda_u z_{7V} - \lambda_t y_{7V}}{\sqrt{2}},$$

$$\tilde{\mathbf{D}} = e^2 G_F d + \frac{D - F}{\sqrt{2}} G_F (\lambda_u z_{7V} - \lambda_t y_{7V})$$

$$\tilde{\mathbf{E}} = \frac{G_F}{\sqrt{2}} \lambda_t y_{7A},$$

$$\tilde{\mathbf{F}} = \frac{D - F}{\sqrt{2}} G_F \lambda_t y_{7A},$$

$$\tilde{\mathbf{K}} = \frac{m_\Sigma + m_p}{q^2 - m_K^2} \sqrt{2} (D - F) G_F \lambda_t y_{7A} m_\mu$$

● Observables may be constructed which are sensitive to terms in the amplitude not dominated by LD contributions

- Such observables are then sensitive to SD effects beyond the SM.

★ Forward-backward asymmetry

$$\mathcal{A}_{\text{FB}} = \frac{\int_{-1}^1 dc_\theta \operatorname{sgn}(c_\theta) \Gamma''}{\int_{-1}^1 dc_\theta \Gamma''}, \quad \Gamma'' = \frac{d^2\Gamma(\Sigma^+ \rightarrow p\mu^+\mu^-)}{dq^2 dc_\theta}, \quad c_\theta = \cos \theta$$

θ angle between μ^- and p directions in dimuon's rest frame

$$\mathcal{A}_{\text{FB}} = \frac{\beta^2 \bar{\lambda}}{64\pi^3 \Gamma' m_\Sigma^3} \operatorname{Re} \left\{ \left[M_+ \tilde{\mathbf{A}}^* \tilde{\mathbf{F}} - M_- \tilde{\mathbf{B}}^* \tilde{\mathbf{E}} - (\tilde{\mathbf{A}}^* \tilde{\mathbf{G}} + \tilde{\mathbf{B}}^* \tilde{\mathbf{H}}) m_\mu + \tilde{\mathbf{C}}^* \tilde{\mathbf{F}} + \tilde{\mathbf{D}}^* \tilde{\mathbf{E}} \right] q^2 \right. \\ \left. - (M_+ \tilde{\mathbf{C}}^* \tilde{\mathbf{G}} - M_- \tilde{\mathbf{D}}^* \tilde{\mathbf{H}}) m_\mu \right\}$$

with $\beta = \sqrt{1 - 4m_\mu^2/q^2}$, $\bar{\lambda} = \hat{m}_-^2 \hat{m}_+^2$, $\hat{m}_\pm^2 = M_\pm^2 - q^2$, $M_\pm = m_\Sigma \pm m_p$

★ Integrated forward-backward asymmetry

$$\tilde{\mathcal{A}}_{\text{FB}} = \frac{1}{\Gamma(\Sigma^+ \rightarrow p\mu^+\mu^-)} \int_{q_{\min}^2}^{q_{\max}^2} dq^2 \int_{-1}^1 dc_\theta \operatorname{sgn}(c_\theta) \Gamma''$$

$$q_{\min}^2 = 4m_\mu^2, \quad q_{\max}^2 = (m_\Sigma - m_p)^2$$

He, JT, Valencia, 1806.08350

★ It's the main observable that could provide a window into NP modifying part of the SM amplitude not dominated by LD effects.

★ Polarization asymmetries of the muons

$$\frac{d\Gamma^-(\varsigma_x^-, \varsigma_y^-, \varsigma_z^-)}{dq^2} = \frac{\Gamma'}{2} (1 + \mathcal{P}_T^- \varsigma_x^- + \mathcal{P}_N^- \varsigma_y^- + \mathcal{P}_L^- \varsigma_z^-)$$

$$\hat{z} = \frac{\mathbf{p}_\mu}{|\mathbf{p}_\mu|}, \quad \hat{y} = \frac{\mathbf{p}_p \times \mathbf{p}_\mu}{|\mathbf{p}_p \times \mathbf{p}_\mu|}, \quad \hat{x} = \hat{y} \times \hat{z}, \quad (\varsigma_x^-)^2 + (\varsigma_y^-)^2 + (\varsigma_z^-)^2 = 1$$

$$\mathcal{P}_L^- = \frac{\beta^2 \sqrt{\lambda}}{192\pi^3 \Gamma' m_\Sigma^3} \text{Re} \left\{ \begin{aligned} &[-3(2M_+ \tilde{A}^* \tilde{E} + \tilde{H}^* \tilde{K}) q^2 - 2(\hat{m}_+^2 + 3q^2) \tilde{C}^* \tilde{E} + 6m_\mu M_+ \tilde{F}^* \tilde{H}] \hat{m}_-^2 \\ &+ [3(2M_- \tilde{B}^* \tilde{F} - \tilde{G}^* \tilde{J}) q^2 - 2(\hat{m}_-^2 + 3q^2) \tilde{D}^* \tilde{F} - 6m_\mu M_- \tilde{E}^* \tilde{G}] \hat{m}_+^2 \end{aligned} \right\}$$

$$\mathcal{P}_N^- = \frac{\beta^2 \bar{\lambda} \sqrt{q^2}}{256\pi^2 \Gamma' m_\Sigma^3} \text{Im} \left\{ \begin{aligned} &2[(M_+ \tilde{A} + \tilde{C})^* \tilde{F} + (\tilde{D} - M_- \tilde{B})^* \tilde{E}] m_\mu - (\tilde{A}^* \tilde{G} + \tilde{B}^* \tilde{H}) q^2 \\ &- (\tilde{C}^* \tilde{G} - \tilde{E}^* \tilde{J}) M_+ + (\tilde{D}^* \tilde{H} - \tilde{F}^* \tilde{K}) M_- \end{aligned} \right\}$$

$$\mathcal{P}_T^- = \frac{\beta \bar{\lambda} \sqrt{q^2}}{256\pi^2 \Gamma' m_\Sigma^3} \text{Re} \left\{ \begin{aligned} &2[2(M_+ \tilde{A} + \tilde{C})^* (\tilde{D} - M_- \tilde{B}) - M_- \tilde{A}^* \tilde{E} + M_+ \tilde{B}^* \tilde{F}] m_\mu \\ &- M_+ \tilde{C}^* \tilde{J} + M_- \tilde{D}^* \tilde{K} + \beta^2 (M_+ \tilde{E}^* \tilde{G} - M_- \tilde{F}^* \tilde{H}) \end{aligned} \right\}$$

$$- \frac{\beta \bar{\lambda} \text{Re} \left[(\tilde{A}^* \tilde{J} + \tilde{B}^* \tilde{K}) q^4 + 2(\tilde{C}^* \tilde{E} + \tilde{D}^* \tilde{F}) M_+ M_- m_\mu \right]}{256\pi^2 \Gamma' m_\Sigma^3 \sqrt{q^2}}$$

He, JT, Valencia, 1806.08350

★ Integrated polarization asymmetries

$$\tilde{P}_{L,N,T}^- = \frac{1}{\Gamma(\Sigma^+ \rightarrow p\mu^+\mu^-)} \int_{q_{\min}^2}^{q_{\max}^2} dq^2 \Gamma' \mathcal{P}_{L,N,T}^-$$

• These muon asymmetries are analogous to those studied in the literature for

■ inclusive $b \rightarrow s\ell^+\ell^-$

Hewett, 1996
Kruger & Sehgal, 1996
Guetta & Nardi, 1998
Fukae, Kim, Morozumi, Yoshikawa, 1999
Fukae, Kim, Yoshikawa, 2000
Bensalem, London, Sinha, Sinha, 2003

■ exclusive decay $\Lambda_b \rightarrow \Lambda\ell^+\ell^-$

Chen & Geng, 2001
Aliev, Ozpineci, Savci, 2003
Giri & Mohanta, 2006

■ rare kaon decays $K \rightarrow \pi\mu^+\mu^-$.

Savage & Wise, 1990
Agrawal, Ng, Belanger, Geng, 1992

- LD contributions dominate \mathcal{P}_T

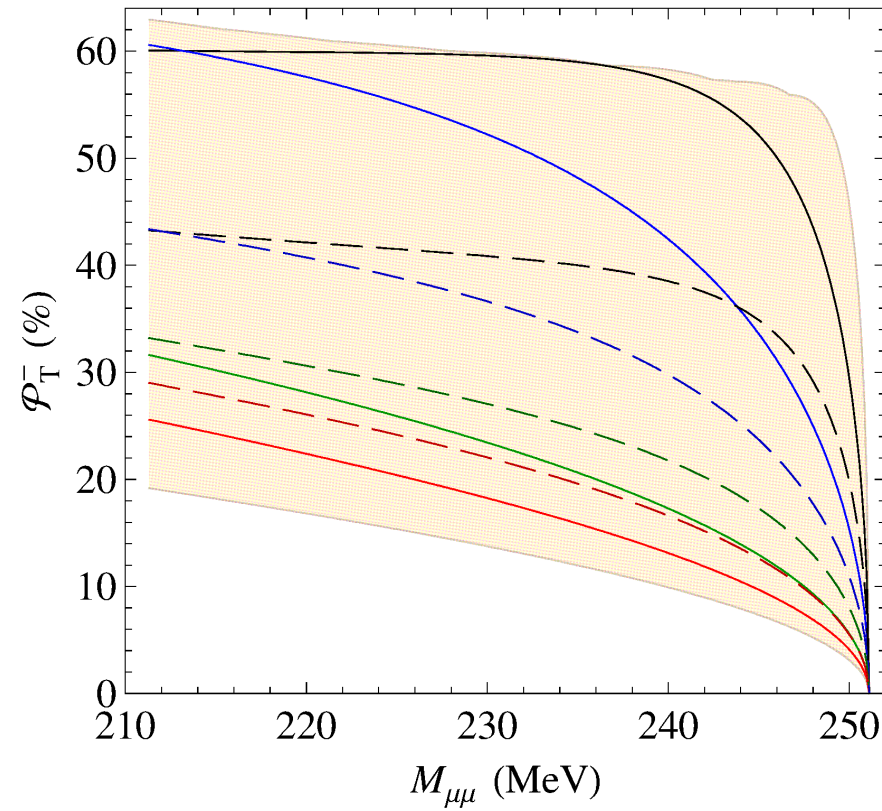


FIG. 3: The μ^- transverse-polarization asymmetry \mathcal{P}_T^- in $\Sigma^+ \rightarrow p\mu^+\mu^-$ versus $M_{\mu\mu}$ in the SM.

He, JT, Valencia, 1806.08350

Branching fraction & asymmetries of $\Sigma^+ \rightarrow p\mu^+\mu^-$ in SM

$\frac{\text{Re } a}{\text{MeV}}$	$\frac{\text{Re } b}{\text{MeV}}$	$10^8 \mathcal{B}$	$10^5 \tilde{A}_{\text{FB}}$	$10^5 \tilde{P}_{\text{L}}^-$	$10^6 \tilde{P}_{\text{N}}^-$	\tilde{P}_{T}^- (%)
13.3	-6.0	1.6	3.7	-7.0	-0.2	59
-13.3	6.0	3.5	-1.4	4.5	-9.6	50
6.0	-13.3	5.1	0.9	-5.1	-1.1	23
-6.0	13.3	9.1	-0.3	3.3	-3.1	17
11.0	-7.4	2.4	2.7	-5.7	-7.3	41
-11.0	7.4	4.7	-0.7	4.1	-10	36
7.4	-11.0	4.0	1.4	-5.2	-5.0	26
-7.4	11.0	7.4	-0.3	3.6	-6.0	21

TABLE I: Sample values of the branching fraction \mathcal{B} of $\Sigma^+ \rightarrow p\mu^+\mu^-$ and the corresponding integrated asymmetries \tilde{A}_{FB} and $\tilde{P}_{\text{L,N,T}}^-$ computed within the SM including the SD and LD contributions. In the evaluation of the \mathcal{B} , \tilde{A}_{FB} , and $\tilde{P}_{\text{L,N,T}}^-$ entries in the first [last] four rows, the relativistic [heavy baryon] expressions for $\text{Im}(a, b, c, d)$ have been used, as explained in the text.

He, JT, Valencia, 1806.08350

Branching fraction & asymmetries of $\Sigma^+ \rightarrow p\mu^+\mu^-$ in SM

$\frac{\text{Re } a}{\text{MeV}}$	$\frac{\text{Re } b}{\text{MeV}}$	$10^8 \mathcal{B}$	$10^5 \tilde{A}_{\text{FB}}$	$10^5 \tilde{P}_{\text{L}}^-$	$10^6 \tilde{P}_{\text{N}}^-$	\tilde{P}_{T}^- (%)
13.3	-6.0	1.6	3.7	-7.0	-0.2	59
-13.3	6.0	3.5	-1.4	4.5	-9.6	50
6.0	-13.3	5.1	0.9	-5.1	-1.1	23
-6.0	13.3	9.1	-0.3	3.3	-3.1	17
11.0	-7.4	2.4	2.7	-5.7	-7.3	41
-11.0	7.4	4.7	-0.7	4.1	-10	36
7.4	-11.0	4.0	1.4	-5.2	-5.0	26
-7.4	11.0	7.4	-0.3	3.6	-6.0	21

TABLE I: Sample values of the branching fraction \mathcal{B} of $\Sigma^+ \rightarrow p\mu^+\mu^-$ and the corresponding integrated asymmetries \tilde{A}_{FB} and $\tilde{P}_{\text{L,N,T}}^-$ computed within the SM including the SD and LD contributions. In the evaluation of the \mathcal{B} , \tilde{A}_{FB} , and $\tilde{P}_{\text{L,N,T}}^-$ entries in the first [last] four rows, the relativistic [heavy baryon] expressions for $\text{Im}(a, b, c, d)$ have been used, as explained in the text.

He, JT, Valencia, 1806.08350

- The asymmetries expected to be tiny in the SM can serve as probes of NP effects
 - These asymmetries are (approximate) null tests of the SM.

Enhanced asymmetries in of $\Sigma^+ \rightarrow p\mu^+\mu^-$ due to new physics

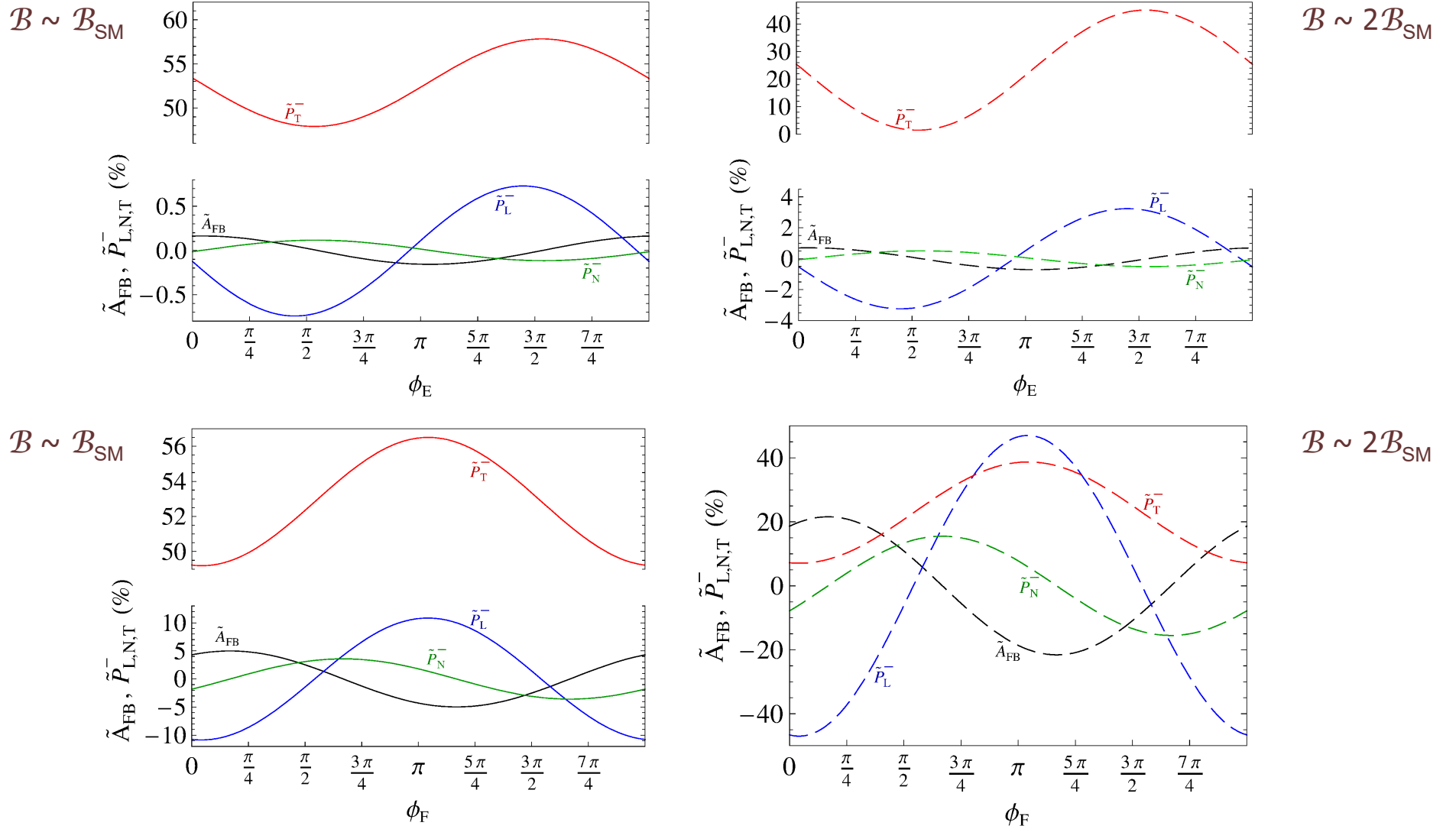


FIG. 4: The integrated asymmetries \tilde{A}_{FB} and $\tilde{P}_{\text{L,N,T}}^{-}$ of the muon in $\Sigma^+ \rightarrow p\mu^+\mu^-$ versus the phases $\phi_{\text{E,F}}$ of the NP contributions to the coefficients \tilde{E} (top plots) and \tilde{F} (bottom plots), respectively, in the decay amplitude. For the top plots, only \tilde{E} has the NP term with magnitude $g_{\text{E}} = 7 \times 10^{-9} \text{ GeV}^{-2}$ (left) and $7 \times 10^{-8} \text{ GeV}^{-2}$ (right). For the bottom plots, only \tilde{F} has the NP term with magnitude $g_{\text{F}} = 1 \times 10^{-8} \text{ GeV}^{-2}$ (left) and $1 \times 10^{-7} \text{ GeV}^{-2}$ (right).

Introduction

$$\Sigma^+ \rightarrow p \mu^+ \mu^-$$

- Flavor-changing baryon decay $\mathcal{B} \rightarrow \mathcal{B}' \nu \nu$

Lepton-number-violating $\mathcal{B}^- \rightarrow \mathcal{B}'^+ \ell^- \ell^-$

Conclusions

$$\mathcal{B} \rightarrow \mathcal{B}' \nu \nu$$

- This decay proceeds mainly from the SD contribution.
- In general $s \rightarrow d \nu \nu$ interactions contribute not only to $K \rightarrow \pi \nu \nu$ but also to $K \rightarrow \nu \nu$ and $\Sigma^+ \rightarrow p \nu \nu$.
 - Constraints from their data are complementary to each other.
- $\mathcal{B}(K_L \rightarrow \nu \nu)_{\text{SM}} \sim 10^{-10}$ and $\mathcal{B}(K_L \rightarrow \nu \nu)_{\text{exp}} < 6.3 \times 10^{-4}$
- $\mathcal{B}(\Sigma^+ \rightarrow p \nu \nu)_{\text{SM}} \sim 5 \times 10^{-13}$

Marciano & Parsa, 1996
Gninenko, 2015

HB Li, 2017

$$B \rightarrow B' \nu \nu$$

- This decay proceeds mainly from the SD contribution.
- In general $s \rightarrow d \nu \nu$ interactions contribute not only to $K \rightarrow \pi \nu \nu$ but also to $K \rightarrow \nu \nu$ and $\Sigma^+ \rightarrow p \nu \nu$.

- Constraints from their data are complementary to each other.

Marciano & Parsa, 1996
Gninenko, 2015

- $\mathcal{B}(K_L \rightarrow \nu \nu)_{\text{SM}} \sim 10^{-10}$ and $\mathcal{B}(K_L \rightarrow \nu \nu)_{\text{exp}} < 6.3 \times 10^{-4}$

HB Li, 2017

- $\mathcal{B}(\Sigma^+ \rightarrow p \nu \nu)_{\text{SM}} \sim 5 \times 10^{-13}$

- Expected BESIII sensitivities with 10^{10} events on the J/ψ peak and 3×10^9 events on the $\psi(2S)$ peak.

HB Li, 2017

Decay mode	Current data $\mathcal{B} (\times 10^{-6})$	Sensitivity $\mathcal{B} (90\% \text{ C.L.}) (\times 10^{-6})$
$\Lambda \rightarrow n \nu \bar{\nu}$	–	< 0.3
$\Sigma^+ \rightarrow p \nu \bar{\nu}$	–	< 0.4
$\Xi^0 \rightarrow \Lambda \nu \bar{\nu}$	–	< 0.8
$\Xi^0 \rightarrow \Sigma^0 \nu \bar{\nu}$	–	< 0.9
$\Xi^- \rightarrow \Sigma^- \nu \bar{\nu}$	–	–*
$\Omega^- \rightarrow \Xi^- \nu \bar{\nu}$	–	< 26.0

Introduction

$$\Sigma^+ \rightarrow p \mu^+ \mu^-$$

Flavor-changing baryon decay $\mathcal{B} \rightarrow \mathcal{B}' \nu \nu$

- Lepton-number-violating $\mathcal{B}^- \rightarrow \mathcal{B}'^+ \ell^- \ell^-$

Conclusions

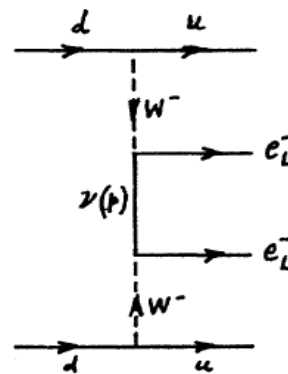
Neutrinoless $\Delta L=2$ hyperon decays

TABLE I. Lepton number violating ($\Delta L = 2$) decays of hyperons. The classification of these decays according to their change in strangeness (ΔS) is also indicated.

Channel	ΔS	Channel	ΔS
$\Sigma^- \rightarrow \Sigma^+ e^- e^-$	0	$\Xi^- \rightarrow p e^- e^-$	2
$\Sigma^- \rightarrow p e^- e^-$	1	$\Xi^- \rightarrow p e^- \mu^-$	2
$\Sigma^- \rightarrow p e^- \mu^-$	1	$\Xi^- \rightarrow p \mu^- \mu^-$	2
$\Sigma^- \rightarrow p \mu^- \mu^-$	1	$\Omega^- \rightarrow \Sigma^+ e^- e^-$	2
$\Xi^- \rightarrow \Sigma^+ e^- e^-$	1	$\Omega^- \rightarrow \Sigma^+ \mu^- e^-$	2
$\Xi^- \rightarrow \Sigma^+ \mu^- e^-$	1	$\Omega^- \rightarrow \Sigma^+ \mu^- \mu^-$	2

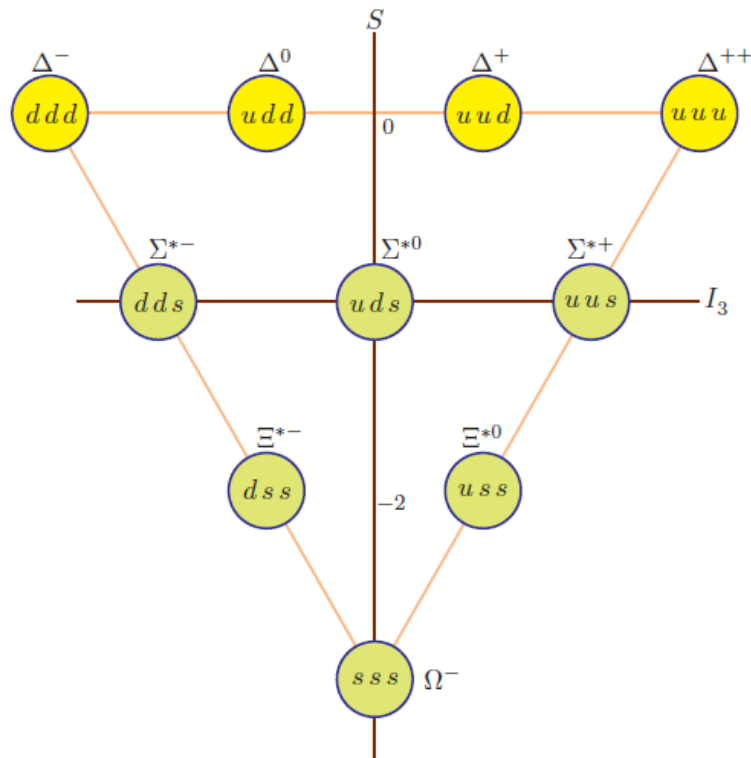
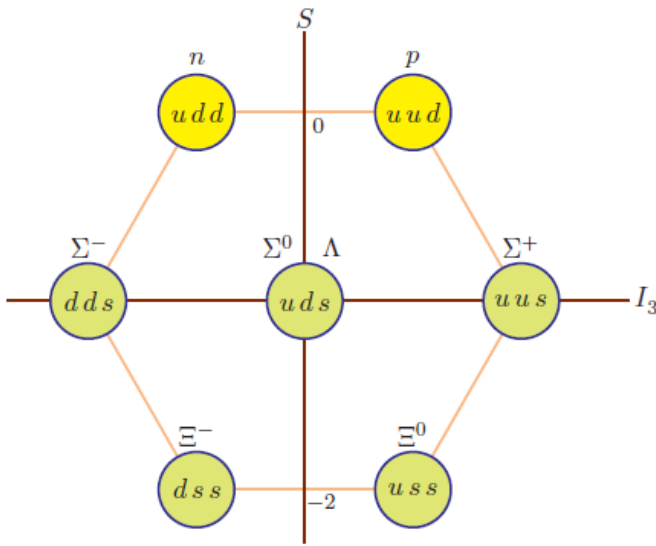
Barbero, Li, Lopez Castro, Mariano, 2013

2 down-type quarks (d or s) convert to $2u + 2\ell^-$



Only experimental limit from HyperCP, 2005

$$B(\Xi^- \rightarrow p \mu^- \mu^-) \leq 4.0 \times 10^{-8}$$



• Loop calculations

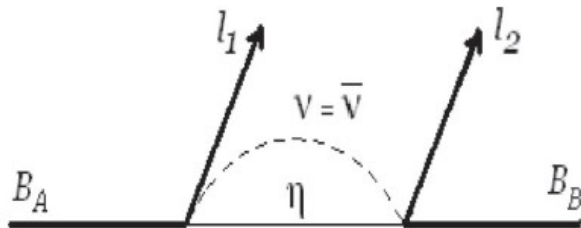


FIG. 1. Feynman graph for $\Delta L = 2$ hyperon decays. The virtual state η denotes an intermediate hyperon state.

TABLE III. Decay rates (normalized to the effective neutrino mass $\langle m_{ll} \rangle^2$) and branching ratios for $\Delta L = 2$ hyperon decays. We use $\langle m_{ee} \rangle^2 = (10 \text{ eV})^2$ and $\langle m_{\mu\mu} \rangle^2 = (10 \text{ MeV})^2$ to evaluate the branching ratios.

	$\Gamma_{0\nu}/\langle m_{ll} \rangle^2$ [$\text{sec}^{-1}/\text{MeV}^2$]	$B(B_A \rightarrow B_B l^- l^-)$
$\Sigma^- \rightarrow \Sigma^+ e^- e^-$	1.000×10^{-15}	1.48×10^{-35}
$\Sigma^- \rightarrow p e^- e^-$	0.497×10^{-10}	7.35×10^{-31}
$\Sigma^- \rightarrow p \mu^- \mu^-$	0.426×10^{-11}	6.31×10^{-20}
$\Xi^- \rightarrow \Sigma^+ e^- e^-$	0.841×10^{-13}	1.38×10^{-33}
$\Xi^- \rightarrow p e^- e^-$	1.150×10^{-12}	1.88×10^{-32}
$\Xi^- \rightarrow p \mu^- \mu^-$	0.480×10^{-12}	7.87×10^{-21}

Barbero, Li, Lopez Castro, Mariano, 2007

• Bag-model method

$$B^{\text{bag}}(\Sigma^- \rightarrow p e^- e^-) \leq 10^{-23}$$

Barbero, Li, Lopez Castro, Mariano, 2013

• Loop calculations

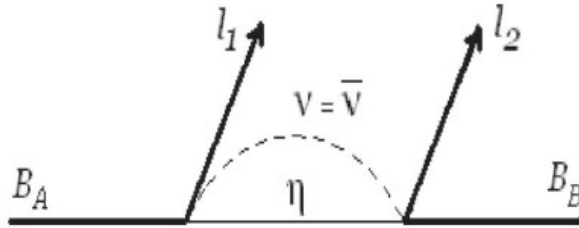


FIG. 1. Feynman graph for $\Delta L = 2$ hyperon decays. The virtual state η denotes an intermediate hyperon state.

TABLE III. Decay rates (normalized to the effective neutrino mass $\langle m_{ll} \rangle^2$) and branching ratios for $\Delta L = 2$ hyperon decays. We use $\langle m_{ee} \rangle^2 = (10 \text{ eV})^2$ and $\langle m_{\mu\mu} \rangle^2 = (10 \text{ MeV})^2$ to evaluate the branching ratios.

	$\Gamma_{0\nu}/\langle m_{ll} \rangle^2$ [$\text{sec}^{-1}/\text{MeV}^2$]	$B(B_A \rightarrow B_B l^- l^-)$
$\Sigma^- \rightarrow \Sigma^+ e^- e^-$	1.000×10^{-15}	1.48×10^{-35}
$\Sigma^- \rightarrow p e^- e^-$	0.497×10^{-10}	7.35×10^{-31}
$\Sigma^- \rightarrow p \mu^- \mu^-$	0.426×10^{-11}	6.31×10^{-20}
$\Xi^- \rightarrow \Sigma^+ e^- e^-$	0.841×10^{-13}	1.38×10^{-33}
$\Xi^- \rightarrow p e^- e^-$	1.150×10^{-12}	1.88×10^{-32}
$\Xi^- \rightarrow p \mu^- \mu^-$	0.480×10^{-12}	7.87×10^{-21}

Barbero, Li, Lopez Castro, Mariano, 2007

• Bag-model method $B^{\text{bag}}(\Sigma^- \rightarrow p e^- e^-) \leq 10^{-23}$

Barbero, Li, Lopez Castro, Mariano, 2013

• Despite the large uncertainties, these numbers suggest that an observation of any of these decays would be good evidence for NP.

- Expected BESIII sensitivities with 10^{10} events on the J/ψ peak and 3×10^9 events on the $\psi(2S)$ peak.

HB Li, 2017

Decay mode	Current data $\mathcal{B} (\times 10^{-6})$	Sensitivity $\mathcal{B} (90\% \text{ C.L.}) (\times 10^{-6})$
$\Sigma^- \rightarrow \Sigma^+ e^- e^-$	–	< 1.0
$\Sigma^- \rightarrow p e^- e^-$	–	< 0.6
$\Xi^- \rightarrow p e^- e^-$	–	< 0.4
$\Xi^- \rightarrow \Sigma^+ e^- e^-$	–	< 0.7
$\Omega^- \rightarrow \Sigma^+ e^- e^-$	–	< 15.0
$\Sigma^- \rightarrow p \mu^- \mu^-$	–	< 1.1
$\Xi^- \rightarrow p \mu^- \mu^-$	< 0.04	< 0.5
$\Omega^- \rightarrow \Sigma^+ \mu^- \mu^-$	–	< 17.0
$\Sigma^- \rightarrow p e^- \mu^-$	–	< 0.8
$\Xi^- \rightarrow p e^- \mu^-$	–	< 0.5
$\Xi^- \rightarrow \Sigma^+ e^- \mu^-$	–	< 0.8
$\Omega^- \rightarrow \Sigma^+ e^- \mu^-$	–	< 17.0

Introduction

$$\Sigma^+ \rightarrow p \mu^+ \mu^-$$

Flavor-changing baryon decay $\mathcal{B} \rightarrow \mathcal{B}' \nu \nu$

Lepton-number-violating $\mathcal{B}^- \rightarrow \mathcal{B}'^+ \ell^- \ell^-$

- Conclusions

- Rare hyperon decays can serve as potentially sensitive probes of physics beyond the SM.
- Concerning BSM physics, these decays can offer useful information which is complementary to that from the kaon sector.
- For $\Sigma^+ \rightarrow p \mu^+ \mu^-$, although the observables in the SM involve significant uncertainties, some of the muon asymmetries are predicted to be tiny in the SM and therefore can be sensitive to BSM physics, which may be testable at LHCb.
- The flavor-changing hyperon decays $B \rightarrow B' \nu \nu$ and lepton-number-violating $B^- \rightarrow B'^+ \ell^- \ell^-$ offer good null tests of the SM, which may be experimentally feasible at BESIII.